

**Figure 1. Germ line knockdown of Hop leads to transposon up-regulation.** *A*, domain organization of Hop. *DP*, dipeptide. *B*, quantitative PCR results showing the extent of Hop mRNA knockdown in two different RNAi lines. *Act5c* ( $\beta$ -actin) was used as internal control, and *Oregon-R* was used as wild-type control. The dotted line represents arbitrary levels of Hop mRNA in control ovaries. Error bars represent mean  $\pm$  S.E. *C*, immunoblotting analysis demonstrating the efficiency of germ line knockdown of Hop. Molecular weight markers are shown on the left. *Act5c* ( $\beta$ -actin) was used as loading control. Two-fold serial dilutions of ovary lysates from control and Hop GLKD ovaries were used. The dotted lines across the immunoblots show the region where nitrocellulose membrane was cut prior to exposure to primary antibody. *D*, morphology of control and Hop GLKD ovaries. Ovaries containing nos.Gal4 driven Luciferase were used as control. For comparison of ovary morphology, ovary from *piwi*<sup>1</sup>/*piwi*<sup>2</sup> flies is shown on the right. *E*, bar plot showing log<sub>2</sub> value of real-fold change from EBSec output. False discovery rate (FDR) cutoff was 0.1. Relative expression of Hop is also shown (box). Consistent with Fig. 1B, Hop mRNA levels were significantly reduced.

ical linker, Hsp70-Hsp90-organizing protein (Hop), which together make up the Hsp90 chaperone machine (29). Recent work has explored epigenetic functions of Hsp90. Hsp90 acts as an evolutionary capacitor of phenotypic variation. In *Drosophila*, inhibition of Hsp83, the Hsp90 ortholog, along with environmental stress both similarly induce morphological changes. Hsp83's role in the maintenance of normal morphology was first deemed a result of Hsp83's stabilization of early development transcription factors and signaling clientele (30). The evolutionary conservation of the Hsp90-Hsp70 chaperone machinery reflects the complexity and specificity of this system's regulatory function. Hundreds of client proteins interact and depend on this system, and it has emerged as an important regulator of epigenetic processes.

Recent studies have shown that Hsp90 and its associated co-chaperones regulate small non-coding RNA pathways. Mutations of the *Drosophila* orthologs of Hsp90 and Hsp70 have been shown to reduce assembly of RNA-induced silencing complexes (RISCs) (31). Our previous work has shown that Hsp90 and Hop interact with Piwi, mediate its phosphorylation, and silence phenotypic variations (32). Hsp90 mediates accurate loading of piRNA precursors into piRNA-binding proteins, and the absence of Hsp90 leads to inefficient piRNA biogenesis with a concurrent increase in TE mobility (33, 34). Further, Shutdown (encoded by *shu*), a member of the FKBP family of immunophilins and an interacting partner of Hsp90, was

shown to be required for both primary and secondary piRNA biogenesis (35, 36). The Shutdown ortholog in mice, FKBP6, is required for secondary piRNA biogenesis (37).

In this study, we show that germ line knockdown (GLKD) of Hop, a Hsp90 co-chaperone, leads to significant up-regulation of transposons, showing that Hop is essential for silencing TE. Like other piRNA pathway mutants (38), Hop GLKD leads to induction of phosphorylation of histone  $\gamma$ -H2Av, a marker for double-strand DNA breaks. Further, Hop GLKD leads to a sterile phenotype where females can lay eggs, but none of the eggs hatch into larvae. We also show that Hop is dispensable for either the stability or the cellular localization of key piRNA pathway proteins, Piwi, Aubergine, Ago3, and Vasa, indicating that Hop functions downstream of these proteins. We finally show that Hop is essential for efficient piRNA biogenesis. Based on these results, we conclude that Hop is critical for the maintenance of genome integrity and that it does so by silencing transposons and regulating piRNA biogenesis.

## Results and discussion

Hop (STIP1 in humans) is the co-chaperone responsible for the transfer of client proteins between Hsp70 and Hsp90. Hop is evolutionarily conserved in eukaryotes, and it localizes to both the nucleus and the cytoplasm (39). Hop is a monomeric protein that consists of three tetratricopeptide repeat domains (TPR1, TPR2A, and TPR2B) and one aspartic acid-pro-

line repeat dipeptide domain (Fig. 1A). The TPR domains interact with the C termini of Hsp90 and Hsp70, with TPR1 and TPR2B binding to Hsp70 and TPR2A binding preferentially to Hsp90. The intermediate structures of heat shock machinery are difficult to characterize completely because of the transient and fast-paced nature of chaperone function (40). The physical transfer process and the conformations involved in Hop's function have yet to be solved.

Previous work had demonstrated that co-chaperone Hop interacts with Piwi and functions in preventing phenotypic variations (32). Further, several heat shock proteins and FKBP6 were shown to interact with mammalian PIWI protein orthologs Miwi and Mili. These results gave us a clue that Hop could potentially play a role in the piRNA pathway. Hence, we decided to characterize the potential role of Hop in the piRNA pathway. To this end, we used RNA interference to knock down Hop specifically in the germ line cells of *Drosophila* ovary using nos.Gal4 (germ line knockdown or GLKD). We tested two different Hop RNAi lines, *Hop*<sup>HMS00779</sup> and *Hop*<sup>HMS00965</sup>, that were generated by the Transgenic RNAi Project (TRiP, Harvard Medical School) (41, 42). Both RNAi lines target Hop mRNA using 21-nt shRNA. Analysis using the Updated Targets of RNAi Reagents (UP-TORR) Fly tool (43) showed that both shRNAs have zero off-target effects. Knockdown using *Hop*<sup>HMS00779</sup> and *Hop*<sup>HMS00965</sup> produced 91 and 25% reduction in Hop mRNA, respectively, when compared with Hop mRNA levels in Oregon-R (wild type) (Fig. 1B). Because *Hop*<sup>HMS00779</sup> was highly efficient in eliminating Hop mRNA, we used this line to characterize the role of Hop in the piRNA pathway. From here on, Hop GLKD refers to *Hop*<sup>HMS00779</sup>.

Hop GLKD greatly reduced the levels of Hop protein in the germ line (Fig. 1C, compare lanes 1–3 with lanes 4–6). We next tested whether Hop GLKD impacted ovary development. Hop GLKD ovaries looked like wild-type counterparts, suggesting that germ line Hop is dispensable for general ovary development (Fig. 1D). However, mothers with Hop GLKD could lay eggs at the same rate as the control, but none of the eggs hatched into larvae (data not shown). Such a phenotype is reminiscent of piRNA pathway mutants where transposon up-regulation leads to severe DNA damage and activation of Chk2 DNA damage checkpoint (38, 44). So we tested whether Hop GLKD leads to activation of transposons. To this end, we performed mRNA-seq with RNA from control and Hop GLKD ovaries. Reads mapping to mRNAs from transposons and genes were quantified using RSEM (45). Differential expression of transposons was analyzed using EBSeq (46). Differentially expressed transposons and genes with false discovery rate < 0.1 were deemed statistically significant. Hop GLKD resulted in statistically significant differential expression of 35 transposons. Of these, 34 were up-regulated and 1 (*Tabor*) was down-regulated (Fig. 1E). This result shows that Hop is essential for transposon silencing. Of the 35 differentially expressed transposons, 24 (~70%) were Group 1 transposons that require Ago3 for silencing (15). These results are not surprising considering that Hop mRNA was knocked down specifically in the germ line but not in the soma. Consistent with this, soma dominant transposons such as *ZAM* and *Idefix* did not make the list of differentially expressed transposons.

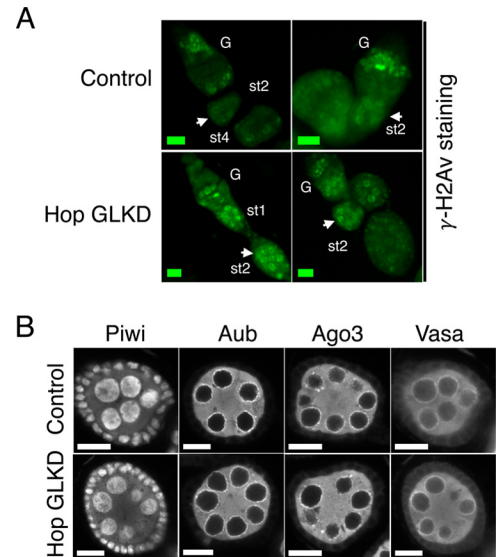


**Figure 2. Effect of Hop GLKD on  $\gamma$ -H2Av accumulation and localization of piRNA pathway proteins.** A, confocal images of two independent ovarioles from control and Hop GLKD flies stained for  $\gamma$ -H2Av. Scale bars are 10  $\mu$ m. G, germarium; st, stage. White arrows point at stage two egg chambers. B, confocal images of stage two egg chambers from control and Hop GLKD ovaries staining for Piwi, Aub, Ago3, and Vasa. Scale bars are 10  $\mu$ m.

Transposon up-regulation in piRNA pathway mutants results in DNA double-strand breaks (DSBs), leading to induction of  $\gamma$ -H2Av (phosphorylated form of histone H2Av) foci (38, 44). DSBs induce phosphorylation of a conserved SQ motif in the C-terminal tail of H2Av (47, 48), and  $\gamma$ -H2Av accumulates near DSBs (49, 50). Because Hop GLKD leads to transposon up-regulation, we tested whether it also leads to induction and accumulation of  $\gamma$ -H2Av foci in the nuclei. Immunofluorescence microscopy showed that, upon Hop GLKD,  $\gamma$ -H2Av foci significantly accumulate in region 3/stage 1 of germarium, and these persist into stage 2 egg chambers and beyond (Fig. 2A, compare white arrows in Control and Hop GLKD panels). These results show that Hop is critical for maintenance of genome integrity and that its absence leads to activation of DNA damage response, presumably due to transposon activation.

We next tested whether Hop GLKD derails transposon silencing by affecting proper cellular localization of key piRNA pathway components, Piwi, Aub, Ago3, and Vasa. In control ovaries, Piwi localized to the nucleus; Aub, Ago3, and Vasa were cytoplasmic and localized to the perinuclear region called the nuage (Fig. 2B, upper panel). This is consistent with earlier findings (6, 15, 51–53). Proper localization of these proteins to their designated cellular spots is critical for both piRNA biogenesis and transposon silencing (11). However, localization of Piwi, Aub, Ago3, and Vasa did not change upon Hop GLKD (Fig. 2B, compare lower panel with upper panel). These results show that Hop is dispensable for proper cellular localization of key piRNA pathway components. Presumably, Hop functions downstream of Piwi, Aub, Ago3, and Vasa. These results are in contrast to the findings in earlier studies where either germ line clones of *shu* or knockdown of *shu* led to significant decrease in the levels and localization of Piwi, Aub, and Ago3 (35, 36). However, this is consistent with *qin* mutants where transposon silencing was



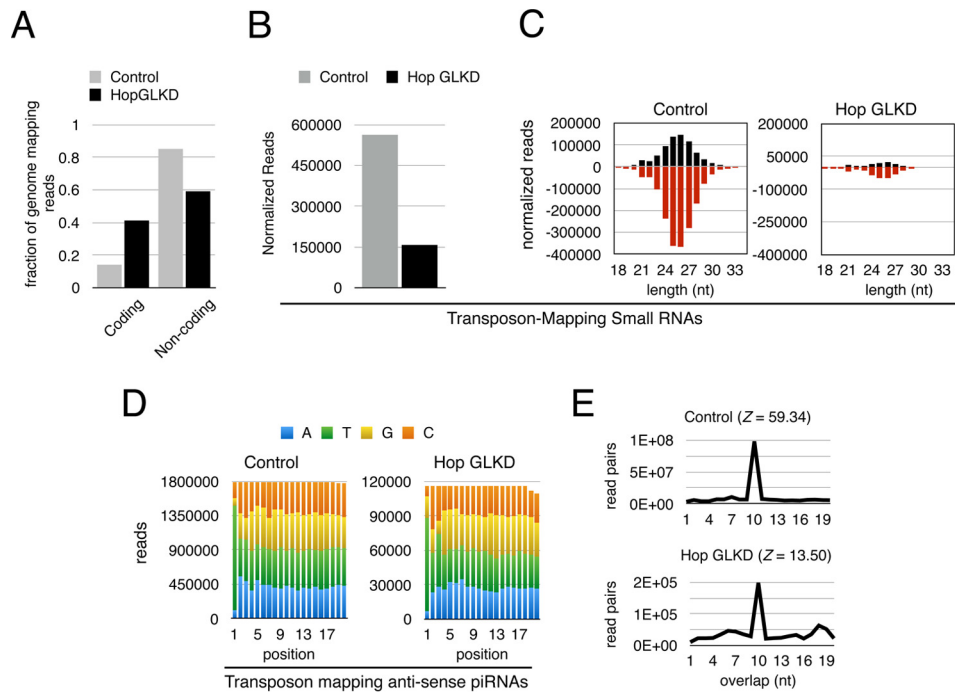


**Figure 3. Hop is required for efficient piRNA biogenesis.** *A*, quantitation of small RNA reads mapping to coding and non-coding portion of the genome in control and Hop GLKD ovaries. *B*, normalized numbers of reads uniquely mapping to transposons are plotted. Reads were normalized to the number of reads mapping to the coding portion of the genome. *C*, length and strand orientation analysis of normalized reads mapping to transposons. Reads were normalized to the number of reads mapping to the coding portion of the genome. *Positive and negative numbers* indicate sense and antisense strands, respectively. *D*, nucleotide composition of first 20 nt of antisense small RNAs mapping to transposons in control and Hop GLKD ovaries. *E*, Ping-Pong analysis for small RNA reads mapping to transposons. *Z*-score is shown in *parentheses*. Notice the preference for 10-nt overlap between sense and antisense reads. Shown on the y axis is the number of read pairs that can be formed between sense and antisense reads mapping to transposons.

derailed without affecting the levels and cellular localization of Piwi, Aub, Ago3, and Vasa proteins (44). Please note that Shutdown (encoded by *shu*) is an Hsp90 co-chaperone like Hop. Qin (encoded by *qin*) is a Tudor domain- and E3 ligase domain-containing protein.

We next tested whether transposon up-regulation in Hop GLKD is due to defective piRNA biogenesis. We deep-sequenced and analyzed small RNAs from Hop GLKD and control ovaries. We first analyzed the composition of genome mapping reads (Fig. 3*A*). Specifically, we quantified reads that mapped to coding and non-coding regions of the genome. In control flies, 14 and 86% of the reads mapped to coding and non-coding regions of the genome, respectively. In contrast, in Hop GLKD ovaries, 41 and 59% of the reads mapped to the coding and non-coding regions, respectively. Thus, there is an ~3-fold increase in the number of small RNAs that map to the coding region of the genome in Hop GLKD when compared with the control. These results show that small RNA biogenesis from the non-coding portion of the genome decreases drastically in Hop GLKD.

Next, we tested whether Hop GLKD affects biogenesis of transposon-mapping small RNAs. We normalized the small RNA libraries in two ways: (*a*) based on the number of reads that uniquely map to the genome and (*b*) based on the number of reads that map to coding regions (supplemental Fig. S1). Both normalization methods showed that Hop GLKD drastically reduced the number of transposon-mapping small RNAs. Specifically, when we normalized based on uniquely mapping genomic reads, we noticed a 50% drop in the number of transposon-mapping small RNAs, and a 72% drop when we normalized based on reads mapping to the coding portion of the genome (Fig. 3*B*). Both sense and antisense transposon-mapping reads showed drastic reduction when compared with the control (Fig. 3*C*). Based on these results, we conclude that Hop is critical for biogenesis of transposon-mapping small RNAs. Because the majority of transposon-mapping small RNAs are 23–29-nt piRNAs, we conclude that Hop is essential for piRNA biogenesis.

To get clues into how Hop regulates piRNA biogenesis, we analyzed the signature of residual piRNAs in Hop GLKD ovaries. We noticed that preference for U as the first nucleotide at the 5' end does not change, showing that 5' end processing of piRNAs remains active in Hop GLKD (Fig. 3*D*, compare *green bars* in *left and right panels*). Further, Ping-Pong cycle mediated by Aub and Ago3 remains active in Hop GLKD as evidenced by the preference for 10-nt overlap in sense and antisense piRNAs (Fig. 3*E*). However, *Z*-score, which is a relative measure of the preference for 10-nt overlap over other length overlaps, significantly decreases from 59.34 in control to 13.50 in Hop GLKD (Fig. 3*E*). The decrease in *Z*-score suggests that Hop GLKD affects the efficiency of Ping-Pong, which can, in turn, affect the accumulation of piRNAs. Inefficient piRNA accumulation, in turn, affects the piRNA pathway's ability to target and destroy transposons.

In summary, we have shown that Hop is essential for transposon silencing and efficient piRNA biogenesis. Hop GLKD leads to transposon activation and induction of DNA damage signaling due to the significant reduction in piRNA levels.

Reduction in the number of piRNAs is due neither to the loss of Piwi, Aub, Ago3, and Vasa nor to the loss of Ping-Pong cycle. It is intriguing to note that Shutdown and Hop, both being TPR domain-containing Hsp90 co-chaperones, exhibit distinct effects upon GLKD. Shutdown GLKD not only affected Piwi proteins' levels and cellular localization, but it also affected fecundity (35, 36). Shutdown GLKD females lay far fewer eggs than control, showing that Shutdown is essential for general ovary development and that piRNA biogenesis is perhaps one of the many functions it performs during ovary development. On the other hand, upon Hop GLKD, ovary development is normal, females lay eggs at the same rate as control, and Piwi proteins' localization is not affected. However, transposon silencing and piRNA biogenesis are affected. In other words, Hop is dispensable for ovary development but is indispensable for transposon silencing and piRNA biogenesis. Perhaps Shutdown and Hop function at distinct stages of the piRNA pathway. We propose that Hop regulates the efficient accumulation of piRNAs. It can function at two distinct stages: (a) it could mediate efficient exchange of sense and antisense precursors between Aub and Ago3, which in turn increases the rate of Ping-Pong cycle, and/or (b) it could function in coordinating post-piRNA biogenesis targeting of transposon mRNAs. Derailment of either of these steps leads to defects in piRNA biogenesis and transposon silencing. Further biochemical and genetic dissection will precisely define the function of Hop in transposon silencing, efficient piRNA biogenesis, and maintenance of genome integrity.

## Experimental procedures

### Fly stocks and handling

All *Drosophila* strains were maintained at 25 °C. The *nos-Gal4* driver fly strain (stock number 32563;  $y^1 w^*$ ;  $P\{GAL4-nos.NGT\}A$ ), Hop shRNA lines *Hop*<sup>HMS00779</sup> (stock number 32979) and *Hop*<sup>HMS00965</sup> (stock number 34002), and control line (stock number 35788,  $P\{UAS-LUC.VALIUM10\}attP2$ ) came from the Bloomington *Drosophila* Stock Center, Bloomington, IN. We refer to the control line as UAS-Luc. The control line had firefly luciferase (Luc) coding sequence inserted at the attP2 site, the same site of insertion as in Hop shRNAs. Both Hop RNAi lines used in Fig. 1B are short hairpin RNAs and are not expected to have any off-target effects. To make sure that both shRNA lines do not have any off-target effects, we used the UP-TORR Fly tool (43). UP-TORR showed that both RNAi lines HMS00779 and HMS00965 do not have any off-target effects. Knockdowns were achieved by crossing 2–5 virgin females from the RNAi lines for Hop with 1–2 males from *nos.Gal4*. Control cross was set up with 1–2 males from *nos.Gal4* and 2–5 virgin females of UAS-Luc. The progeny from the control cross are referred to as *nos.Luc*. The parental generation was then transferred to new fly food every 4 days. As the F1 generation was born, they were collected, and then put on yeast for 1–2 days for preparation for ovary dissection. Egg hatch rate calculation was performed as described earlier (36) except that apple juice-agar plates were used.

### Ovary lysate preparation and Western blotting analysis

Ten pairs of ovaries from 2–3-day-old yeast-fed females were dissected and homogenized in an Eppendorf tube in 50  $\mu$ l of lysis buffer (20 mM HEPES, pH 7.5, 100 mM KCl, 5 mM MgCl<sub>2</sub>, 0.1% SDS, 0.1% sodium deoxycholate, 1% Triton X-100, 1 mM DTT, and 5% glycerol). The homogenate was then mixed with 50  $\mu$ l of 2 $\times$  Laemmli Sample Buffer (Bio-Rad product number 1610737), boiled at 95 °C for 3 min, and then processed for Western blotting analysis using standard molecular biology techniques.

### Immunostaining and microscopy

*Drosophila* ovaries were manually dissected in ice-cold PBS and fixed with 4% formaldehyde (Electron Microscopy Sciences, Hatfield, PA) as described before (54). Fixed ovary tissues were incubated at 4 °C overnight with primary antibodies at the following concentrations: anti-Piwi (1:500), anti-Ago3 (1:250), anti-Aub (1:1000), anti-Vasa (1:50), and anti- $\gamma$ -H2Av (1:500). Piwi, Aub, and Ago3 antibodies were kind gifts from Dr. Mikiko Siomi (Keio University, Minato, Tokyo, Japan) and Haifan Lin (Yale University). Anti-vasa antibody was deposited to the Developmental Studies Hybridoma Bank (DSHB) by Spradling, A. C./Williams, D. (DSHB Hybridoma Product anti-vasa). Anti- $\gamma$ -H2Av (UNC93-5.2.1) was deposited to the DSHB by Hawley, R. S. (DSHB Hybridoma Product UNC93-5.2.1). Alexa Fluor-conjugated secondary antibodies from Thermo Fisher Scientific were used at 1:500. Confocal images were captured using a Zeiss LSM 880 NLO microscope and Plan-Apochromat 63 $\times$ /1.40 Oil differential interference contrast objective with identical settings for GLKD and control fly lines. Images were analyzed using Fiji (ImageJ) (55). Ovary morphology images shown in Fig. 1D were captured using a Moticam 10 camera mounted on a Zeiss Stemi 2000-C stereo microscope.

### mRNA-seq

Total RNA was isolated using TRIzol Reagent (Ambion) from 10–15 pairs of manually dissected ovaries and stored at –80 °C until use. Two biological repeats of *nos.Luc* (control) and Hop GLKD were used. RNA integrity was verified on an Agilent 2200 TapeStation (Agilent Technologies, Palo Alto, CA). 100–200 ng of total RNA was used to prepare RNA-Seq libraries using the TruSeq RNA Sample Prep Kit following the protocol described by the manufacturer (Illumina, San Diego, CA). Please note that poly(A)-containing RNA was first purified prior to the library preparation step. Single end 50-bp sequencing was performed on an Illumina HiSeq2500. Sequencing was performed at the Hollings Cancer Center Genomics Core Lab at Medical University of South Carolina (MUSC).

### Small RNA-seq

Thirty  $\mu$ g of total RNA from *nos.Luc* (control) and Hop GLKD ovaries was resolved on a 15% denaturing polyacrylamide gel containing 7 M urea. Small RNAs ranging from 20 to 40 nt were purified without oxidation step as described elsewhere (15). Small RNA sequencing libraries were prepared using the TruSeq Small RNA Library Preparation Kit (Illumina)

## ACCELERATED COMMUNICATION: *Hop* and piRNA pathway

with one minor modification. A terminator block oligonucleotide (5'-TAC AAC CCT CAA CCA TAT GTA GTC CAA GCA/3SpC3/-3') was added prior to 5' adapter ligation as described elsewhere (56). This step specifically blocked reverse transcription of 30-nt-long 2S rRNA and hence substantially reduced rRNA contamination in the final sequenced reads. Sequencing libraries were size-selected with a Pippin Prep (Sage Science, Beverly, MA). Single end 36- or 50-bp sequencing was performed on a HiSeq2500 (Illumina). Sequencing was performed at the Hollings Cancer Center Genomics Core Lab at MUSC.

### Quantitative PCR

cDNA preparation was performed using the High-Capacity cDNA Reverse Transcription Kit (Thermo Fisher Scientific) using the manufacturer's protocol. Quantitative PCR was performed using iQ SYBR Green Supermix (Bio-Rad) and a CFX384 Touch Real-Time PCR Detection System (Bio-Rad). Data analysis was performed using Apple Numbers. The following primers were used: (a) 5'-AAGTTGCTGCTCTGGTTGTCG-3' and 5'-GCCACACGCAGCTCATTGTAG-3' for Act5c and (b) 5'-CATTCGCCAAGGCTGGAAAG-3' and 5'-GGGATCGTACTTGAGACCCCTC-3' for Hop.

### Bioinformatics

**mRNA-seq analysis**—Our mRNA-seq analysis was inspired by the piPipes workflow (57). Raw mRNA-seq reads from Illumina HiSeq 2500 were aligned to *Drosophila* (version 5, *dm3*) transcriptome and reference transposon sequences using Bowtie 2 (58, 59) and then quantified by RSEM (45). *dm3* transcriptome (mRNA sequences) was obtained from the UCSC table browser (60), and reference transposon sequences were obtained from FlyBase. Differential expression analysis of transcripts was then performed using EBSeq (46). Differentially expressed transcripts with a false discovery rate < 0.1 were deemed significant.

**Small RNA-seq analysis**—Raw small RNA sequencing reads were processed by cutadapt to remove the 3'-sequencing adapter (TGGAATTCTCGGGTGCCAAGG). Trimmed reads smaller than 18 nt and also the reads without sequencing adapter were discarded. Reads were then depleted of rRNA reads and then aligned to *dm3* genome using Bowtie (59). rRNA mapping allowed two mismatches, and genomic alignment allowed no mismatches. Only reads that perfectly matched the genome were collected and further analyzed. Reads were then collapsed using Perl script *TBr2\_collapse.pl* available as a part of NGS Toolbox (61). Reads were then mapped to mRNA sequences of RefSeq genes without any mismatches using Bowtie and then plotted as fraction of genome mapping reads in Fig. 3A. To compare reads between different samples, the normalization factor was calculated in two ways: (a) based on the number of uniquely mapping genomic reads and (b) based on the number of reads mapping to mRNA sequences of RefSeq genes (protein-coding portion of the genome). Reads were then mapped to transposon consensus sequences using Bowtie 2, and the numbers of reads that align uniquely were noted. The numbers of transposon-mapping reads in Hop GLKD were then multiplied by normalization factor and plotted as shown in

Fig. 3B. To analyze size distribution and nucleotide composition of reads, we mapped reads to transposon consensus sequences using sRNAmapper (62) with default parameters. Under default parameters, sRNAmapper does not allow any mismatch in the first 18 nt from the 5' end of piRNAs and at most allows one mismatch in the rest of the sequence. Size distribution, orientation, and nucleotide composition of such aligned reads were analyzed using Perl script *checkmap.pl*. Output was then exported to Apple Numbers and plotted as shown in Fig. 3, C and D. Ping-Pong signature was analyzed using Perl script *TBr2\_pingpong.pl*. *TBr2\_pingpong.pl* performs Ping-Pong signature analysis and Z-score calculation in the same way as described elsewhere (44). The output of *TBr2\_pingpong.pl* was exported to Apple Numbers and plotted as shown in Fig. 3E. All Perl scripts are available upon request.

---

**Author contributions**—J. A. K. and V. K. G. conceived the project and wrote the manuscript. J. A. K. performed most of the experiments. R. Y. P. performed immunostaining of Piwi proteins and Vasa. D. N. performed immunostaining of  $\gamma$ -H2Av. D. R. wrote all Perl scripts used in this study. V. K. G. performed bioinformatic analysis with help from D. R.

---

**Acknowledgments**—We thank Mikiko Siomi and Haifan Lin for antibodies, members of the Gangaraju lab for critical reading of the manuscript, Robert Wilson and Jennifer Schulte for preparing mRNA and small RNA sequencing libraries, and Philip Zamore and Bo Han for answering our queries during installation and execution of piPipes. We acknowledge support of the Genomics/shRNA Shared Resource and National Institutes of Health Grant P30 CA138313 to Cell & Molecular Imaging Shared Resource, Hollings Cancer Center, Medical University of South Carolina.

---

### References

1. Ghildiyal, M., and Zamore, P. D. (2009) Small silencing RNAs: an expanding universe. *Nat. Rev. Genet.* **10**, 94–108
2. Ishizu, H., Siomi, H., and Siomi, M. C. (2012) Biology of PIWI-interacting RNAs: new insights into biogenesis and function inside and outside of germlines. *Genes Dev.* **26**, 2361–2373
3. Juliano, C., Wang, J., and Lin, H. (2011) Uniting germline and stem cells: the function of Piwi proteins and the piRNA pathway in diverse organisms. *Annu. Rev. Genet.* **45**, 447–469
4. Kim, V. N., Han, J., and Siomi, M. C. (2009) Biogenesis of small RNAs in animals. *Nat. Rev. Mol. Cell Biol.* **10**, 126–139
5. Siomi, M. C., Sato, K., Pezic, D., and Aravin, A. A. (2011) PIWI-interacting small RNAs: the vanguard of genome defence. *Nat. Rev. Mol. Cell Biol.* **12**, 246–258
6. Brennecke, J., Aravin, A. A., Stark, A., Dus, M., Kellis, M., Sachidanandam, R., and Hannon, G. J. (2007) Discrete small RNA-generating loci as master regulators of transposon activity in *Drosophila*. *Cell* **128**, 1089–1103
7. Das, P. P., Bagijn, M. P., Goldstein, L. D., Woolford, J. R., Lehrbach, N. J., Sapetschnig, A., Buhecha, H. R., Gilchrist, M. J., Howe, K. L., Stark, R., Matthews, N., Berezikov, E., Ketting, R. F., Tavaré, S., and Miska, E. A. (2008) Piwi and piRNAs act upstream of an endogenous siRNA pathway to suppress Tc3 transposon mobility in the *Caenorhabditis elegans* germline. *Mol. Cell* **31**, 79–90
8. Houwing, S., Kamminga, L. M., Berezikov, E., Cronembold, D., Girard, A., van den Elst, H., Filippov, D. V., Blaser, H., Raz, E., Moens, C. B., Plasterk, R. H., Hannon, G. J., Draper, B. W., and Ketting, R. F. (2007) A role for Piwi and piRNAs in germ cell maintenance and transposon silencing in Zebrafish. *Cell* **129**, 69–82



9. Vagin, V. V., Sigova, A., Li, C., Seitz, H., Gvozdev, V., and Zamore, P. D. (2006) A distinct small RNA pathway silences selfish genetic elements in the germline. *Science* **313**, 320–324
10. Pane, A., Wehr, K., and Schüpbach, T. (2007) *zucchini* and *squash* encode two putative nucleases required for rasiRNA production in the *Drosophila* germline. *Dev. Cell* **12**, 851–862
11. Malone, C. D., Brennecke, J., Dus, M., Stark, A., McCombie, W. R., Sachidanandam, R., and Hannon, G. J. (2009) Specialized piRNA pathways act in germline and somatic tissues of the *Drosophila* ovary. *Cell* **137**, 522–535
12. Czech, B., Preall, J. B., McGinn, J., and Hannon, G. J. (2013) A transcriptome-wide RNAi screen in the *Drosophila* ovary reveals factors of the germline piRNA pathway. *Mol. Cell* **50**, 749–761
13. Handler, D., Meixner, K., Pizka, M., Lauss, K., Schmied, C., Gruber, F. S., and Brennecke, J. (2013) The genetic makeup of the *Drosophila* piRNA pathway. *Molecular cell* **50**, 762–777
14. Gunawardane, L. S., Saito, K., Nishida, K. M., Miyoshi, K., Kawamura, Y., Nagami, T., Siomi, H., and Siomi, M. C. (2007) A slicer-mediated mechanism for repeat-associated siRNA 5' end formation in *Drosophila*. *Science* **315**, 1587–1590
15. Li, C., Vagin, V. V., Lee, S., Xu, J., Ma, S., Xi, H., Seitz, H., Horwich, M. D., Syrzycka, M., Honda, B. M., Kittler, E. L., Zapp, M. L., Klattenhoff, C., Schulz, N., Theurkauf, W. E., et al. (2009) Collapse of germline piRNAs in the absence of Argonaute3 reveals somatic piRNAs in flies. *Cell* **137**, 509–521
16. Nishimasu, H., Ishizu, H., Saito, K., Fukuhara, S., Kamatani, M. K., Bonfond, L., Matsumoto, N., Nishizawa, T., Nakanaga, K., Aoki, J., Ishitani, R., Siomi, H., Siomi, M. C., and Nureki, O. (2012) Structure and function of Zucchini endoribonuclease in piRNA biogenesis. *Nature* **491**, 284–287
17. Ipsaro, J. J., Haase, A. D., Knott, S. R., Joshua-Tor, L., and Hannon, G. J. (2012) The structural biochemistry of Zucchini implicates it as a nuclease in piRNA biogenesis. *Nature* **491**, 279–283
18. Hayashi, R., Schnabl, J., Handler, D., Mohn, F., Ameres, S. L., and Brennecke, J. (2016) Genetic and mechanistic diversity of piRNA 3'-end formation. *Nature* **539**, 588–592
19. Han, B. W., Wang, W., Li, C., Weng, Z., and Zamore, P. D. (2015) Non-coding RNA. piRNA-guided transposon cleavage initiates Zucchini-dependent, phased piRNA production. *Science* **348**, 817–821
20. Mohn, F., Handler, D., and Brennecke, J. (2015) Noncoding RNA. piRNA-guided slicing specifies transcripts for Zucchini-dependent, phased piRNA biogenesis. *Science* **348**, 812–817
21. Han, B. W., Hung, J. H., Weng, Z., Zamore, P. D., and Ameres, S. L. (2011) The 3'-to-5' exoribonuclease Nibbler shapes the 3' ends of microRNAs bound to *Drosophila* Argonaute1. *Curr. Biol.* **21**, 1878–1887
22. Liu, N., Abe, M., Sabin, L. R., Hendriks, G. J., Naqvi, A. S., Yu, Z., Cherry, S., and Bonini, N. M. (2011) The exoribonuclease Nibbler controls 3' end processing of microRNAs in *Drosophila*. *Curr. Biol.* **21**, 1888–1893
23. Wang, H., Ma, Z., Niu, K., Xiao, Y., Wu, X., Pan, C., Zhao, Y., Wang, K., Zhang, Y., and Liu, N. (2016) Antagonistic roles of Nibbler and Hen1 in modulating piRNA 3' ends in *Drosophila*. *Development* **143**, 530–539
24. Feltzin, V. L., Khaladkar, M., Abe, M., Parisi, M., Hendriks, G. J., Kim, J., and Bonini, N. M. (2015) The exonuclease Nibbler regulates age-associated traits and modulates piRNA length in *Drosophila*. *Aging Cell* **14**, 443–452
25. Eddy, E. M. (1974) Fine structural observations on the form and distribution of nuage in germ cells of the rat. *Anat. Rec.* **178**, 731–757
26. Qi, H., Watanabe, T., Ku, H. Y., Liu, N., Zhong, M., and Lin, H. (2011) The Yb body, a major site for Piwi-associated RNA biogenesis and a gateway for Piwi expression and transport to the nucleus in somatic cells. *J. Biol. Chem.* **286**, 3789–3797
27. Schisa, J. A. (2014) Effects of stress and aging on ribonucleoprotein assembly and function in the germ line. *Wiley Interdiscip. Rev. RNA* **5**, 231–246
28. Trepel, J., Mollapour, M., Giaccone, G., and Neckers, L. (2010) Targeting the dynamic HSP90 complex in cancer. *Nat. Rev. Cancer* **10**, 537–549
29. Alvira, S., Cuéllar, J., Röhl, A., Yamamoto, S., Itoh, H., Alfonso, C., Rivas, G., Buchner, J., and Valpuesta, J. M. (2014) Structural characterization of the substrate transfer mechanism in Hsp70/Hsp90 folding machinery mediated by Hop. *Nat. Commun.* **5**, 5484
30. Queitsch, C., Sangster, T. A., and Lindquist, S. (2002) Hsp90 as a capacitor of phenotypic variation. *Nature* **417**, 618–624
31. Iwasaki, S., Sasaki, H. M., Sakaguchi, Y., Suzuki, T., Tadakuma, H., and Tomari, Y. (2015) Defining fundamental steps in the assembly of the *Drosophila* RNAi enzyme complex. *Nature* **521**, 533–536
32. Gangaraju, V. K., Yin, H., Weiner, M. M., Wang, J., Huang, X. A., and Lin, H. (2011) *Drosophila* Piwi functions in Hsp90-mediated suppression of phenotypic variation. *Nat. Genet.* **43**, 153–158
33. Izumi, N., Kawaoka, S., Yasuhara, S., Suzuki, Y., Sugano, S., Katsuma, S., and Tomari, Y. (2013) Hsp90 facilitates accurate loading of precursor piRNAs into PIWI proteins. *RNA* **19**, 896–901
34. Specchia, V., Piacentini, L., Tritto, P., Fanti, L., D'Alessandro, R., Palumbo, G., Pimpinelli, S., and Bozzetti, M. P. (2010) Hsp90 prevents phenotypic variation by suppressing the mutagenic activity of transposons. *Nature* **463**, 662–665
35. Olivieri, D., Senti, K. A., Subramanian, S., Sachidanandam, R., and Brennecke, J. (2012) The cochaperone shutdown defines a group of biogenesis factors essential for all piRNA populations in *Drosophila*. *Mol. Cell* **47**, 954–969
36. Preall, J. B., Czech, B., Guzzardo, P. M., Muerdter, F., and Hannon, G. J. (2012) *shutdown* is a component of the *Drosophila* piRNA biogenesis machinery. *RNA* **18**, 1446–1457
37. Xiol, J., Cora, E., Kogelgruber, R., Chuma, S., Subramanian, S., Hosokawa, M., Reuter, M., Yang, Z., Berninger, P., Palencia, A., Benes, V., Penninger, J., Sachidanandam, R., and Pillai, R. S. (2012) A role for Fkbp6 and the chaperone machinery in piRNA amplification and transposon silencing. *Mol. Cell* **47**, 970–979
38. Klattenhoff, C., Bratu, D. P., McGinnis-Schultz, N., Koppetsch, B. S., Cook, H. A., and Theurkauf, W. E. (2007) *Drosophila* rasiRNA pathway mutations disrupt embryonic axis specification through activation of an ATR/Chk2 DNA damage response. *Dev. Cell* **12**, 45–55
39. Schmid, A. B., Lagleder, S., Gräwert, M. A., Röhl, A., Hagn, F., Wandinger, S. K., Cox, M. B., Demmer, O., Richter, K., Groll, M., Kessler, H., and Buchner, J. (2012) The architecture of functional modules in the Hsp90 co-chaperone Sti1/Hop. *EMBO J.* **31**, 1506–1517
40. Yamamoto, S., Subedi, G. P., Hanashima, S., Satoh, T., Otaka, M., Wakui, H., Sawada, K., Yokota, S., Yamaguchi, Y., Kubota, H., and Itoh, H. (2014) ATPase activity and ATP-dependent conformational change in the co-chaperone HSP70/HSP90-organizing protein (HOP). *J. Biol. Chem.* **289**, 9880–9886
41. Ni, J. Q., Markstein, M., Binari, R., Pfeiffer, B., Liu, L. P., Villalta, C., Booker, M., Perkins, L., and Perrimon, N. (2008) Vector and parameters for targeted transgenic RNA interference in *Drosophila melanogaster*. *Nat. Methods* **5**, 49–51
42. Perkins, L. A., Holderbaum, L., Tao, R., Hu, Y., Sopko, R., McCall, K., Yang-Zhou, D., Flockhart, I., Binari, R., Shim, H. S., Miller, A., Housden, A., Foos, M., Randkvel, S., Kelley, C., et al. (2015) The Transgenic RNAi Project at Harvard Medical School: Resources and Validation. *Genetics* **201**, 843–852
43. Hu, Y., Roesel, C., Flockhart, I., Perkins, L., Perrimon, N., and Mohr, S. E. (2013) UP-TORR: online tool for accurate and up-to-date annotation of RNAi Reagents. *Genetics* **195**, 37–45
44. Zhang, Z., Xu, J., Koppetsch, B. S., Wang, J., Tipping, C., Ma, S., Weng, Z., Theurkauf, W. E., and Zamore, P. D. (2011) Heterotypic piRNA Ping-Pong requires Qin, a protein with both E3 ligase and Tudor domains. *Mol. Cell* **44**, 572–584
45. Li, B., and Dewey, C. N. (2011) RSEM: accurate transcript quantification from RNA-Seq data with or without a reference genome. *BMC Bioinformatics* **12**, 323
46. Leng, N., Dawson, J. A., Thomson, J. A., Ruotti, V., Rissman, A. I., Smits, B. M., Haag, J. D., Gould, M. N., Stewart, R. M., and Kendziorski, C. (2013) EBSeq: an empirical Bayes hierarchical model for inference in RNA-seq experiments. *Bioinformatics* **29**, 1035–1043
47. Madigan, J. P., Chotkowski, H. L., and Glaser, R. L. (2002) DNA double-strand break-induced phosphorylation of *Drosophila* histone variant H2Av helps prevent radiation-induced apoptosis. *Nucleic Acids Res.* **30**, 3698–3705

## ACCELERATED COMMUNICATION: *Hop and piRNA pathway*

48. Rogakou, E. P., Pilch, D. R., Orr, A. H., Ivanova, V. S., and Bonner, W. M. (1998) DNA double-stranded breaks induce histone H2AX phosphorylation on serine 139. *J. Biol. Chem.* **273**, 5858–5868
49. Modesti, M., and Kanaar, R. (2001) DNA repair: spot(light)s on chromatin. *Curr. Biol.* **11**, R229–232
50. Redon, C., Pilch, D., Rogakou, E., Sedelnikova, O., Newrock, K., and Bonner, W. (2002) Histone H2A variants H2AX and H2AZ. *Curr. Opin. Genet. Dev.* **12**, 162–169
51. Cox, D. N., Chao, A., and Lin, H. (2000) piwi encodes a nucleoplasmic factor whose activity modulates the number and division rate of germline stem cells. *Development* **127**, 503–514
52. Saito, K., Nishida, K. M., Mori, T., Kawamura, Y., Miyoshi, K., Nagami, T., Siomi, H., and Siomi, M. C. (2006) Specific association of Piwi with rasiRNAs derived from retrotransposon and heterochromatic regions in the *Drosophila* genome. *Genes Dev.* **20**, 2214–2222
53. Lim, A. K., and Kai, T. (2007) Unique germ-line organelle, nuage, functions to repress selfish genetic elements in *Drosophila melanogaster*. *Proc. Natl. Acad. Sci. U.S.A.* **104**, 6714–6719
54. Lin, H., and Spradling, A. C. (1993) Germline stem cell division and egg chamber development in transplanted *Drosophila* germlaria. *Dev. Biol.* **159**, 140–152
55. Schindelin, J., Arganda-Carreras, I., Frise, E., Kaynig, V., Longair, M., Pietzsch, T., Preibisch, S., Rueden, C., Saalfeld, S., Schmid, B., Tinevez, J. Y., White, D. J., Hartenstein, V., Eliceiri, K., Tomancak, P., and Cardona, A. (2012) Fiji: an open-source platform for biological-image analysis. *Nat. Methods* **9**, 676–682
56. Wickersheim, M. L., and Blumenstiel, J. P. (2013) Terminator oligo blocking efficiently eliminates rRNA from *Drosophila* small RNA sequencing libraries. *BioTechniques* **55**, 269–272
57. Han, B. W., Wang, W., Zamore, P. D., and Weng, Z. (2015) piPipes: a set of pipelines for piRNA and transposon analysis via small RNA-seq, RNA-seq, degradome- and CAGE-seq, ChIP-seq and genomic DNA sequencing. *Bioinformatics* **31**, 593–595
58. Langmead, B., and Salzberg, S. L. (2012) Fast gapped-read alignment with Bowtie 2. *Nat. Methods* **9**, 357–359
59. Langmead, B., Trapnell, C., Pop, M., and Salzberg, S. L. (2009) Ultrafast and memory-efficient alignment of short DNA sequences to the human genome. *Genome Biol.* **10**, R25
60. Karolchik, D., Hinrichs, A. S., Furey, T. S., Roskin, K. M., Sugnet, C. W., Haussler, D., and Kent, W. J. (2004) The UCSC Table Browser data retrieval tool. *Nucleic Acids Res.* **32**, D493–496
61. Rosenkranz, D., Han, C. T., Roovers, E. F., Zischler, H., and Ketting, R. F. (2015) Piwi proteins and piRNAs in mammalian oocytes and early embryos: from sample to sequence. *Genom. Data* **5**, 309–313
62. Roovers, E. F., Rosenkranz, D., Mahdipour, M., Han, C. T., He, N., Chuva de Sousa Lopes, S. M., van der Westerlaken, L. A., Zischler, H., Butter, F., Roelen, B. A., and Ketting, R. F. (2015) Piwi proteins and piRNAs in mammalian oocytes and early embryos. *Cell Rep.* **10**, 2069–2082